



Primary Retroperitoneal Masses: A Pictorial Essay

Abhishek Gupta¹ Alpana Manchanda¹ Sapna Singh¹ Rajdeep Singh² Nita Khurana³
Aishwarya S. Durgad¹

¹ Department of Radiology, Maulana Azad Medical College, Delhi, India

² Department of Surgery, Maulana Azad Medical College, Delhi, India

³ Department of Pathology, Maulana Azad Medical College, Delhi, India

Address for correspondence Alpana Manchanda, MBBS, MD,
Department of Radiology, Maulana Azad Medical College, Delhi
110002, India (e-mail: alpanamanchanda@gmail.com).

J Gastrointestinal Abdominal Radiol ISGAR 2024;7:65–72.

Abstract

Keywords

- retroperitoneal space
- primary retroperitoneal masses
- multidetector computed tomography

Primary retroperitoneal masses include a diverse and uncommon group of lesions that arise within the retroperitoneal space, but do not originate from any retroperitoneal organs. The majority of the lesions are malignant and imaging plays a pivotal role in the detection, staging, and preoperative planning. The evaluation of primary retroperitoneal masses is often challenging owing to the unfamiliarity with the common imaging features of various diseases affecting it. This article describes the multidetector computed tomography appearance of some primary retroperitoneal masses.

Introduction

Primary retroperitoneal masses may be categorized as solid or cystic and range from benign to aggressive in behavior. Benign and malignant masses should be distinguished whenever possible to avoid unnecessary surgical procedures.

Ultrasonography (USG) is the imaging modality performed initially due to its wide availability, ease of performance, low cost, and absence of radiation exposure. It plays an important role in characterization of mass lesions present in the retroperitoneum based on its location, size, shape, extent, margins, solid or cystic nature, echotexture, presence of calcification, and vascularity of the lesion on color Doppler. Presence of any free fluid and associated abnormality in any solid organ or enlarged lymph nodes can also be detected. However, USG examination of the retroperitoneum may be technically limited because of excessive bowel gas or body habitus.

Multidetector computed tomography (CT) plays an important role in depicting the exact compartmental localization of

the masses into five retroperitoneal spaces, which include the anterior pararenal space, posterior pararenal space, perirenal space, central vascular space, and iliopsoas space.¹ It is currently the imaging modality of choice for the evaluation of morphology, internal characterization, assessment of disease extent, and involvement of vessels including the adjacent and distant structures.² It allows excellent reconstructions in planes other than the original scanning plane. Isotropic multiplanar reconstructions of thin overlapping slices in the coronal and sagittal plane provide excellent delineation of the location and extent of retroperitoneal masses.

The appearance of retroperitoneal lesions on cross-sectional imaging may pose a diagnostic challenge to the radiologist. Awareness of specific components of masses, tumor vascularity, and specific patterns of spread helps in further narrowing the differential diagnosis. Therefore, having knowledge of radiological features of various masses on cross-sectional imaging offers valuable insights for differential diagnosis of retroperitoneal masses and their management.

article published online
August 31, 2023

DOI <https://doi.org/10.1055/s-0043-1774296>.
ISSN 2581-9933.

© 2023. The Author(s).

This is an open access article published by Thieme under the terms of the Creative Commons Attribution License, permitting unrestricted use, distribution, and reproduction so long as the original work is properly cited. (<https://creativecommons.org/licenses/by/4.0/>)
Thieme Medical and Scientific Publishers Pvt. Ltd., A-12, 2nd Floor, Sector 2, Noida-201301 UP, India

Normal Anatomy of Retroperitoneum

The retroperitoneum extends from the diaphragm to the pelvis. It extends between the posterior parietal peritoneum anteriorly and the fascia transversalis posteriorly.² The retroperitoneum is divided into the anterior pararenal space, posterior pararenal space, perirenal space, central vascular space, and iliopsoas space¹ (►Fig. 1).

The anterior pararenal space contains the pancreas, duodenum, and a part of the ascending and descending colons. Kidneys, adrenal glands, blood vessels, lymphatics, and ureters are in perirenal spaces. Fat is only present in the posterior pararenal spaces. The central vascular compartment is located between the two perirenal spaces, behind the anterior pararenal space and in front of the spine. It extends from D12 to the L4–L5 vertebra and contains the inferior vena cava (IVC) and its afferent vasculature, abdominal aorta and its branches, lymphatic chains, and the abdominal sympathetic trunk. The iliopsoas compartment contains the psoas major, iliacus, and psoas minor muscles. Although the iliopsoas compartment is behind the transversalis fascia, it is still considered retroperitoneal because it is frequently involved in processes that begin in the retroperitoneum.¹

The anterior and posterior pararenal spaces merge inferiorly, forming the infrarenal retroperitoneal space, which communicates with the prevesical space and extraperitoneal compartments of the pelvis. Because of loose connective tissue in the retroperitoneum, tumors can have widespread extension before clinical presentation.³

Solid primary retroperitoneal masses are broadly classified according to the tissue of origin. Four broad categories include mesodermal, neurogenic, germ cell, and lymphoid masses (►Table 1).³

Cystic primary retroperitoneal masses are classified into neoplastic masses and non-neoplastic masses (►Table 2).³

Malignant Retroperitoneal Tumors

In this section, we will review the imaging features of some common and uncommon malignant retroperitoneal masses such as malignant lymphoma, liposarcoma, myxofibrosarcoma (MFS), extra-adrenal neuroblastoma (NBL), and extra-skeletal Ewing's sarcoma.

Lymphoma

Lymphoma is the most common malignant retroperitoneal neoplasm, as well as being the most common small round cell tumor,⁴ and typically presents as infiltrative homogeneous hypovascular masses around the aorta or IVC, extending between and encasing structures without compressing them.⁵ Upliftment of the great vessels results in “floating aorta” or “CT angiogram” sign (►Fig. 2). Abdominal lymphomas are classified into solitary mass type, multiple nodular type, and diffuse type.⁶ ¹⁸F-fluorodeoxyglucose (¹⁸F-FDG) positron emission tomography (PET)/CT is the standard examination for the diagnosis, staging, and in-treatment evaluation of lymphoma.⁴ Heterogeneous or rim enhancement of lymph nodes due to necrosis with calcifications is seen following radiochemotherapy.⁷ The main differential diagnosis for lymphomatous lymph nodes is tuberculosis.⁶ Mesenteric lymph nodes are more commonly involved in tuberculosis. It is often associated with tuberculous peritonitis, which is characterized by omental caking, smudged mesentery, and high-density ascites. Mesenteric lymph nodes are not commonly involved in Hodgkin's disease. CT shows homogenous enhancement of the enlarged lymph nodes with fewer calcifications in untreated lymphoma

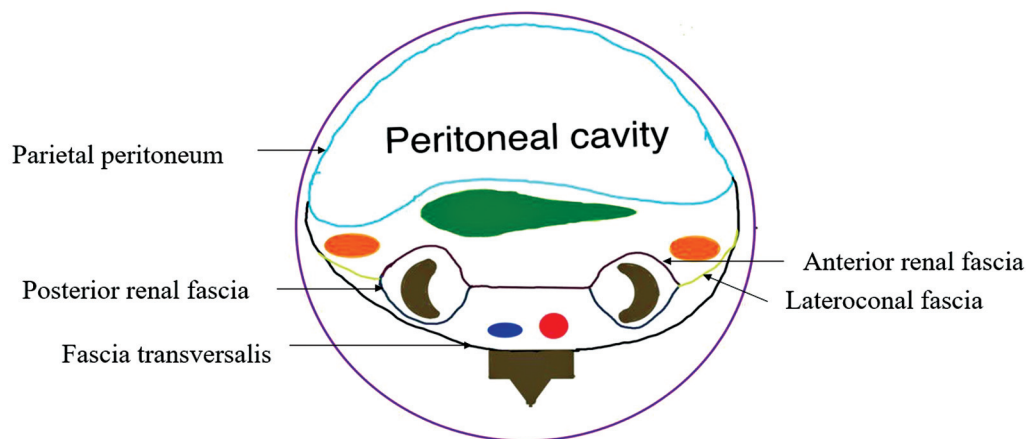


Fig. 1 Schematic diagram of retroperitoneal spaces. The *anterior pararenal space* lies between the anterior renal fascia and parietal peritoneum. It contains the pancreas, duodenum, and the ascending–descending colon. The *perirenal space* lies between the anterior renal fascia and the posterior renal fascia and contains kidneys, adrenal glands, ureters, blood vessels, and lymphatics. The *posterior pararenal space* lies between the fascia transversalis and the posterior renal fascia. The space only contains fat. The *central vascular space* extends from D12 to L4–L5, located between the two perirenal spaces, behind the anterior pararenal space, and in front of the spine. It contains the abdominal aorta and its branches, the inferior vena cava and its afferent vasculature, lymphatic chains, and the abdominal sympathetic trunk. The *iliopsoas space* lies posterior to the fascia transversalis and is generally considered to be retroperitoneal even though it is behind the transversalis fascia because it is frequently involved in processes that begin in the retroperitoneum.

Table 1 Classification of common solid primary retroperitoneal masses according to the tissue of origin

Tissue of origin	Malignant masses	Benign masses
a) Mesodermal		
Adipocytic	Liposarcoma	Lipoma
Smooth muscle	Leiomyosarcoma	Leiomyoma
Striated muscle	Rhabdomyosarcoma	Rhabdomyoma
Connective tissue	Malignant fibrous histiocytoma, chondrosarcoma, synovial cell sarcoma, and fibrosarcoma	Fibroma
b) Neurogenic		
Nerve sheath	Malignant nerve sheath tumors	Schwannoma and neurofibroma
Chromaffin tissue	Malignant paraganglioma or pheochromocytoma	Paraganglioma and pheochromocytoma
Sympathetic nerves	Neuroblastoma	Ganglioneuroma and ganglioneuroblastoma
c) Germ cell neoplasms Embryonic tissue	Teratoma (malignant) and primary extragonadal germ cell tumor (seminomatous and nonseminomatous)	Teratoma (mature and immature)
d) Lymphoid	–	Lymphoma

Table 2 Classification of common cystic primary retroperitoneal masses

Type of mass and origin	Mass
a) Neoplastic	
Mesothelial Germ cell Epithelial	Mesothelioma, cystic teratoma, mucinous cystadenoma or cystadenocarcinoma, serous cystadenocarcinoma
Cystic change in solid neoplasm	Paraganglioma, neurilemoma, and sarcoma
b) Non-neoplastic	
	Hematoma, urinoma, and lymphocele

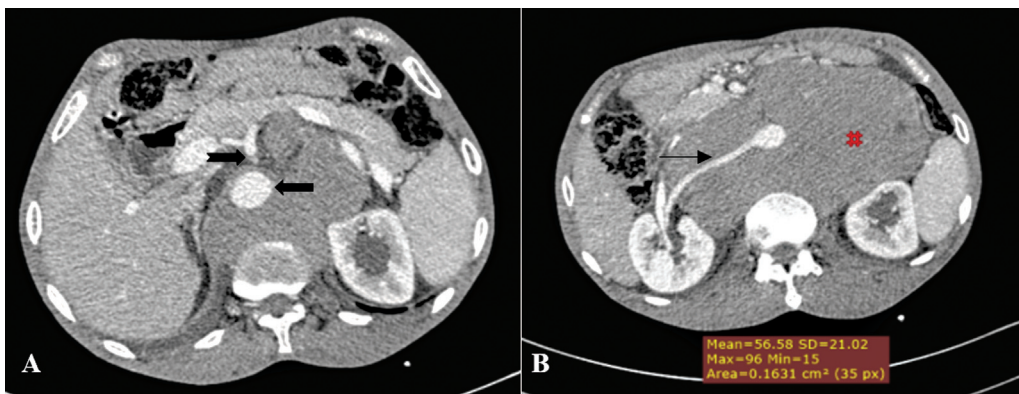


Fig. 2 (A,B) Axial contrast-enhanced computed tomography (CT) of the abdomen in a 55-year-old man shows a homogeneously enhancing mass lesion in the central vascular space of the retroperitoneum causing anterior and lateral displacement of the pancreas and bowel loops, respectively. The lesion is closely abutting the liver, spleen, and bilateral kidneys. It is encasing the aorta and displacing it anteriorly giving the “floating aorta sign” (arrows in A), celiac trunk (notched arrow in A), right renal artery (thin arrow in B). On histopathology, it was proven to be a lymphoma of diffuse large B-cell type (DLBCL).

cases. Peritoneal and omental lymphomatosis is not often seen.⁶

Liposarcoma

Liposarcomas are mesenchymal tumors arising from adipose tissue. Retroperitoneal liposarcomas are classified into five groups: well-differentiated liposarcoma, myxoid liposarcoma, round cell liposarcoma, pleomorphic liposarcoma, and dedifferentiated liposarcoma.⁸

Well-differentiated liposarcomas appear as well-defined fat containing masses with thin septa (►Fig. 3). Calcifications or ossifications within a liposarcoma have proved to be a sign of poor prognosis, often indicating dedifferentiation.⁹ Well-differentiated liposarcomas almost always undergo dedifferentiation,⁸ which is suggested by the additional presence of a focal, nodular nonlipomatous region greater than 1 cm in size (►Fig. 4).¹⁰ Calcification is an important sign of dedifferentiation.³ Myxoid liposarcomas appear as hypoechoic masses on USG. On CT and magnetic resonance imaging (MRI), myxoid liposarcomas have a “pseudocystic” appearance³ due to the extracellular myxoid matrix. They appear as low-attenuation masses in comparison to muscle on CT with bright T2 signal on corresponding MRI. Slowly progressive reticular type of contrast enhancement is seen following contrast administration³ (►Fig. 5), a feature that distinguishes these lesions from a cystic mass.¹⁰ Round cell liposarcoma and pleomorphic liposarcoma exhibit soft-tissue tumor attenuation and signal intensity with a minimal amount of fat.⁸

Myxofibrosarcoma

MFS are fibroblastic lesions that show a spectrum of cellularity, mitotic activity, and nuclear pleomorphism ranging from hypocellular lesions with minimal cytological atypia to more cellular lesions.¹¹ Low-grade MFS invariably show more than 75% myxoid change.¹² They have the unusual characteristic of extending along the fascial planes well

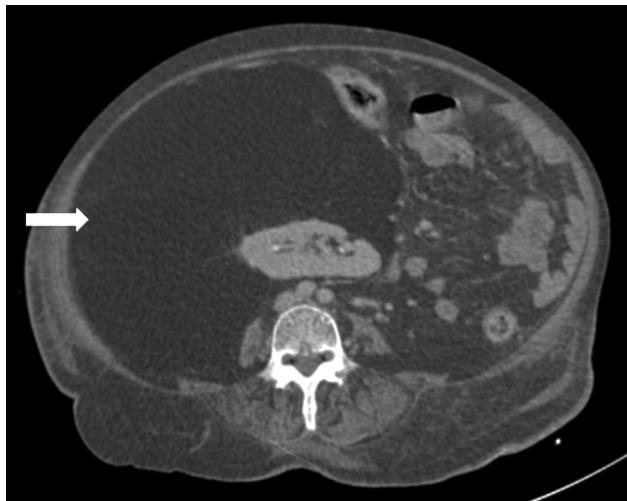


Fig. 3 Axial contrast-enhanced computed tomography (CT) of the abdomen shows a large retroperitoneal mass of fat attenuation (arrow) displacing the right kidney. On histopathology, it proved to be a well-differentiated liposarcoma.



Fig. 4 Axial contrast-enhanced computed tomography (CT) of the abdomen shows a well-defined solid enhancing mass with few areas of fat density (arrow) and multiple enhancing vessels (thin arrow) in the left anterior pararenal space of the retroperitoneum. It was diagnosed as *dedifferentiated liposarcoma* on histopathology.

beyond the primary center of the lesion.¹³ Tail sign, which is defined by the tendency of the tumor to spread along the fascial planes in a curvilinear fashion, seen on MRI is a moderately sensitive and specific sign for MFS.¹² Tail sign is not only valuable for suggesting the diagnosis of MFS but its recognition is also essential in preoperative planning for complete tumor resection (►Fig. 6).

Extra-Adrenal Neuroblastoma

NBL, ganglioneuroblastoma, and ganglioneuroma are tumors of ganglion cell origin derived from the primordial neural crest cells.¹⁴ The most common primary site for NBL is

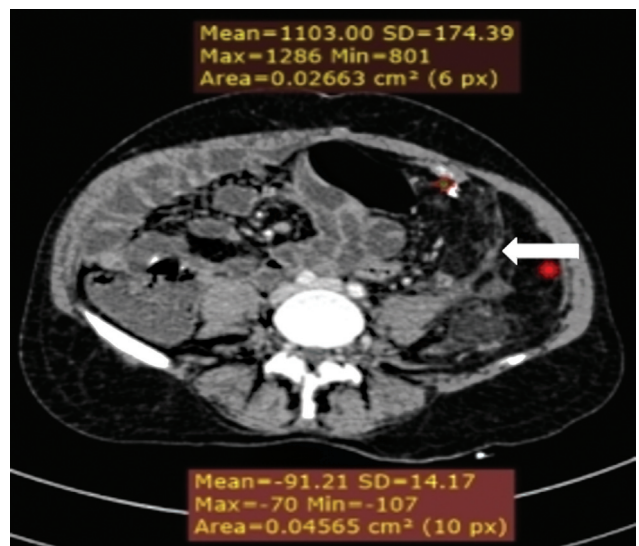


Fig. 5 In another patient, axial contrast-enhanced computed tomography (CT) shows an ill-defined diffusely infiltrative multicompartmental lesion of fat attenuation in the left lumbar and iliac region showing internal fat stranding, eccentric coarse calcifications, and enhancing nodular septations (arrow). It was proven to be *myxoid liposarcoma* on histopathology.

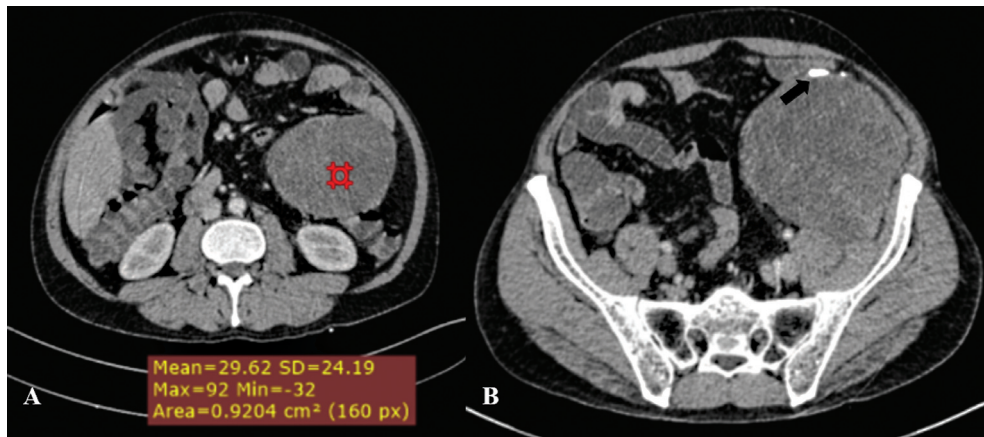


Fig. 6 (A,B) Axial contrast enhanced computed tomography (CT) of the abdomen in a 50-year-old male shows a large heterogeneously enhancing abdominopelvic mass lesion with thin septa, calcification (arrow in B). The mass is abutting the left iliopsoas muscle with loss of intervening fat planes posteriorly. On histopathology, it was proven to be a low-grade myxofibrosarcoma. The red square symbol in figure 6A shows the attenuation of the mass, the parameters of which are given in the box below.

adrenal medulla (35%) and the extra-adrenal paraspinal ganglia (30–35%).¹⁵ NBLs are heterogenous poorly circumscribed masses. Eighty percent to 90% show coarse, amorphous, and mottled calcifications (►Fig. 7).¹⁶ They can demonstrate extension across the midline and into adjacent body cavities. Vascular invasion is not a feature of NBLs.¹⁷

Extraskelatal Ewing's Sarcoma

Extraskelatal Ewing's sarcoma (EES) can occur anywhere in the body and can be classified into central/trunk and peripheral/extremity. On imaging, EESs show extensive necrosis and hemorrhage. Calcification is uncommon in EES. Tumors in the abdomen tend to have infiltrative margins with invasion of the adjacent structures and displace adjacent structures rather than encase them (►Fig. 8). Retroperitoneal EESs are difficult to differentiate from other retroperitoneal tumors in adults such as the renal cell carcinoma and adrenocortical carcinoma. Features in favor of EESs are their earlier age of presentation, absence of metastatic lymphadenopathy, and calcification. Abdominal EESs are mostly unilateral and do not cross the midline.¹⁸

Benign Retroperitoneal Tumors

In this section, we will review the imaging features of some benign retroperitoneal masses like teratoma, paraganglioma, schwannoma, and urinoma.

Teratoma

Teratomas may be composed of mature or immature tissues deriving from the three pluripotent germ cell layers.¹⁹ Mature cystic teratomas (MCTs) are characterized as cystic tumors with fat attenuation and Rokitansky's protuberance.²⁰ Rokitansky's nodules are soft-tissue protuberance within the cyst cavity. Bone or teeth, if present, tend to be located with Rokitansky's nodule (►Fig. 9).²¹ Immature teratomas (ITs) contain variable quantities of immature neural tissue. On cross-sectional imaging, ITs appear as large solid masses containing coarse calcifications and small foci of fat with concomitant hemorrhage.²² Chemotherapy treatment of ITs can result in tissue maturation. This phenomenon is called "retroconversion"; the ITs look more like MCTs.²³ CT findings suggesting maturation are increasing density of tumor masses, appearance of some cystic components, fatty

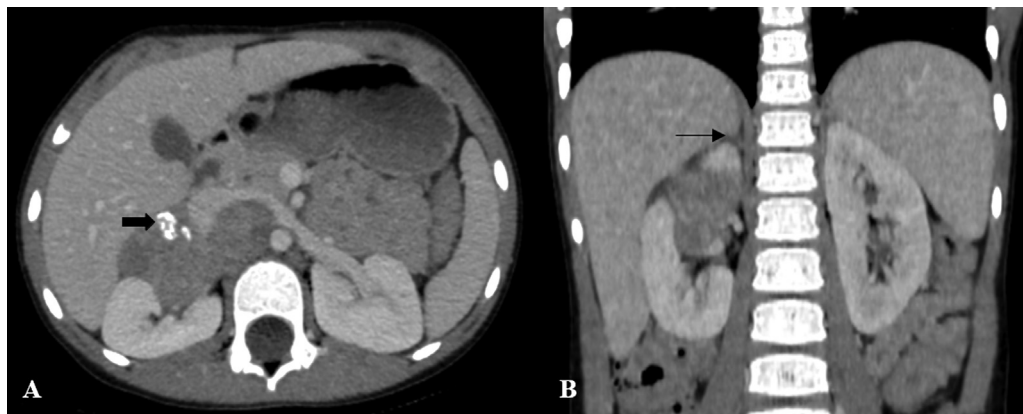


Fig. 7 (A,B) Axial and coronal contrast-enhanced computed tomography (CT) of the abdomen in a 4-year-old girl shows an ill-defined heterogeneously enhancing soft-tissue mass with internal foci of coarse calcifications (arrow in A) centered in the right anterior pararenal space of the retroperitoneum displacing the inferior vena cava (IVC), left renal vein, and pancreas anteriorly. No foci of fat attenuation are noted. No spinal canal extension was noted. The right adrenal gland is normal (thin line arrow in B). It was a proven case of extra-adrenal neuroblastoma.

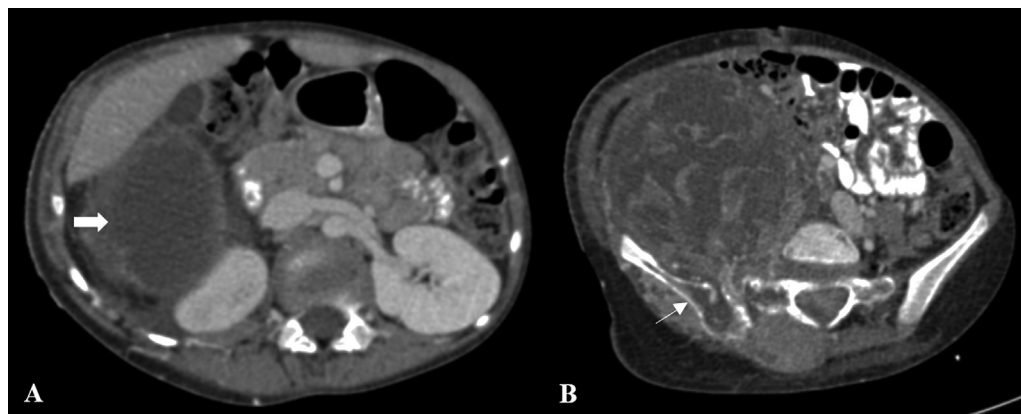


Fig. 8 (A,B) Axial contrast-enhanced computed tomography (CT) of the abdomen in an 11-year-old girl shows a large right-sided abdominopelvic heterogeneously enhancing predominantly cystic retroperitoneal mass lesion (arrow in A) with extensions into the neural foramina and spinal canal, bony destruction, and lytic vertebral lesions (thin arrow in B). On histopathology, it was proven to be extraskeletal Ewing's sarcoma.

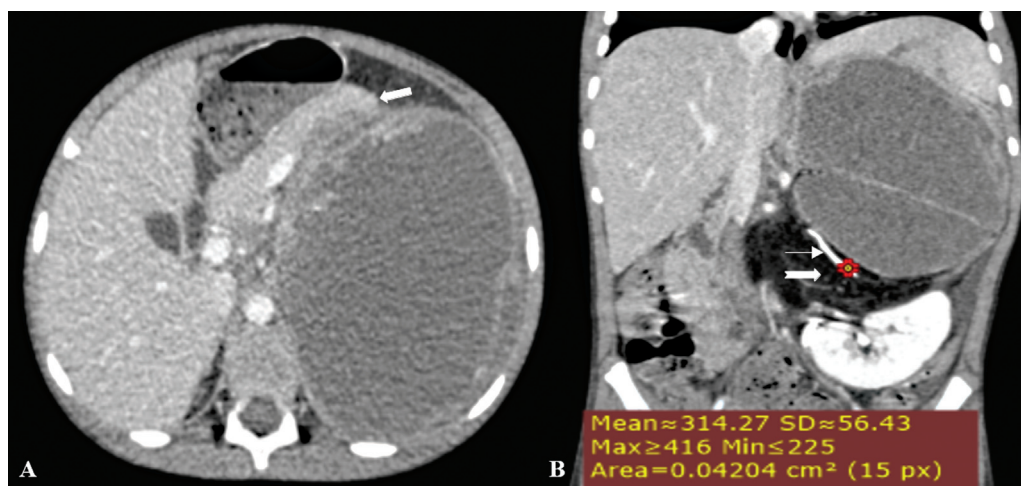


Fig. 9 (A,B) Axial and coronal contrast-enhanced computed tomography (CT) of the abdomen reveals a large heterogenous predominantly cystic retroperitoneal mass lesion causing anterior displacement of the stomach and pancreas (arrow in A) with areas of fat (notched arrow in B) and calcification (mean ~ 314 HU; thin arrow in B) in the left hypochondrium and lumbar regions. Coronal reformatted CT image (B) showing superolateral displacement of the spleen, mass effect, and inferior displacement of the left kidney. On histopathology, it was confirmed to be a mature cystic teratoma.

areas, and curvilinear and punctate calcifications. These masses do not invade the surrounding soft tissues or bone but may gradually compress them.²⁴

Paraganglioma

Paragangliomas are rare tumors of chromaffin cell origin, arising from the extra-adrenal paraganglion cells of sympathetic or parasympathetic nervous systems. The most common site of paragangliomas in the abdomen is the organ of Zuckerkandl located in the para-aortic region near the origin of the inferior mesenteric artery (→Fig. 10).²⁵ They appear as heterogeneous masses with necrosis, hemorrhage, and/or calcifications. Avid contrast material enhancement is often noted because of their hypervascular nature, especially peripheral.²⁶ On T2-weighted MRI, paragangliomas show diffuse high signal intensity known as “lightbulb” sign.

Schwannoma

Schwannomas are benign nerve sheath tumors of Schwann cell origin. On cross-sectional imaging, schwannomas are well-circumscribed masses, most commonly located in the paravertebral or presacral location. Target sign is seen on MRI, consisting of a central low to intermediate T2-signal intensity due to fibrous tissue surrounded by a peripheral high signal intensity of myxoid tissue.²⁷ It may be seen in both schwannomas and neurofibromas. Larger schwannomas are more likely to undergo degenerative changes, which include cyst formation, calcification, hemorrhage, and hyalinization (→Fig. 11).²⁵ Ancient schwannoma refers to a long-standing lesion with advanced degenerative changes.³

Urinoma

Urinoma is a collection of extravasated urine that is found secondary to trauma or iatrogenic causes. They appear

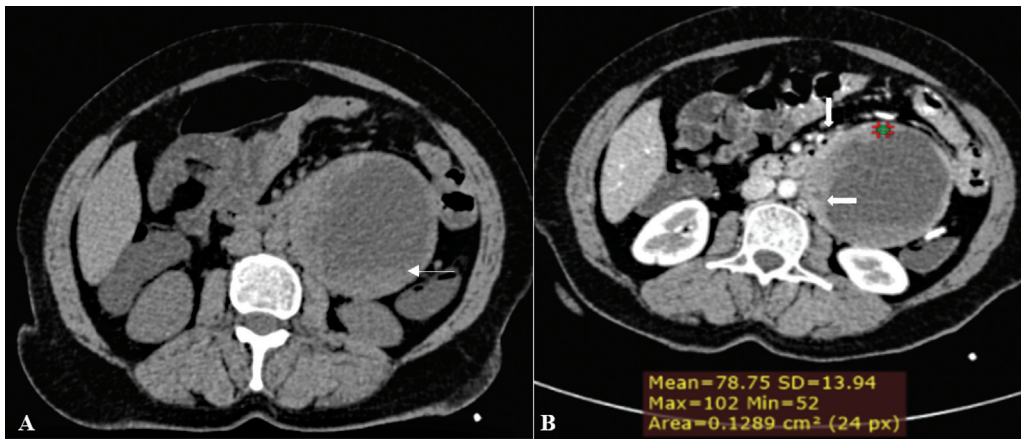


Fig. 10 Axial (A) noncontrast and (B) contrast-enhanced computed tomography (CT) of the abdomen in a 50-year-old woman reveals a well-defined multiloculated solid cystic lesion located in the left paraaortic location at the level of the origin of the inferior mesenteric artery showing fluid–fluid level (*thin arrow* in A) and a hyperenhancing solid component (*arrow* in B). Anterosuperiorly, the mass is seen to abut the fourth part of the duodenum and duodenojejunal junction displacing it anteriorly (*vertical arrow* in B). On histopathology, it was proven to be a *paraganglioma*.

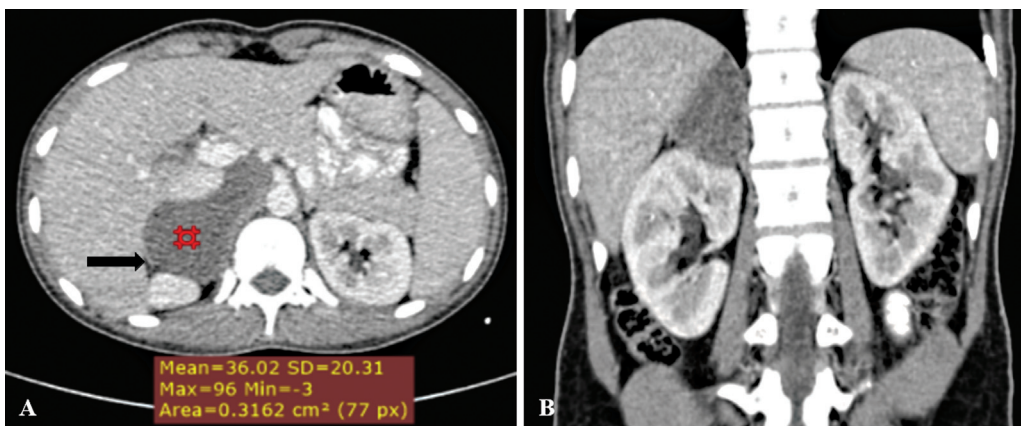


Fig. 11 (A,B) Axial contrast-enhanced computed tomography (CECT) of the abdomen in a 17-year-old adolescent girl shows a large well-defined nonenhancing (mean ~ 38 HU on CECT and 32 on noncontrast-enhanced computed tomography [NCCT], plain scan not shown) lesion in the right suprarenal region. No peripheral rim enhancement or enhancing soft-tissue component is seen. The lesion does not show any focus of fat/calcification within. The right adrenal gland is seen separately from the lesion (*arrow* in A). On histopathology, it was proven to be a *schwannoma*.

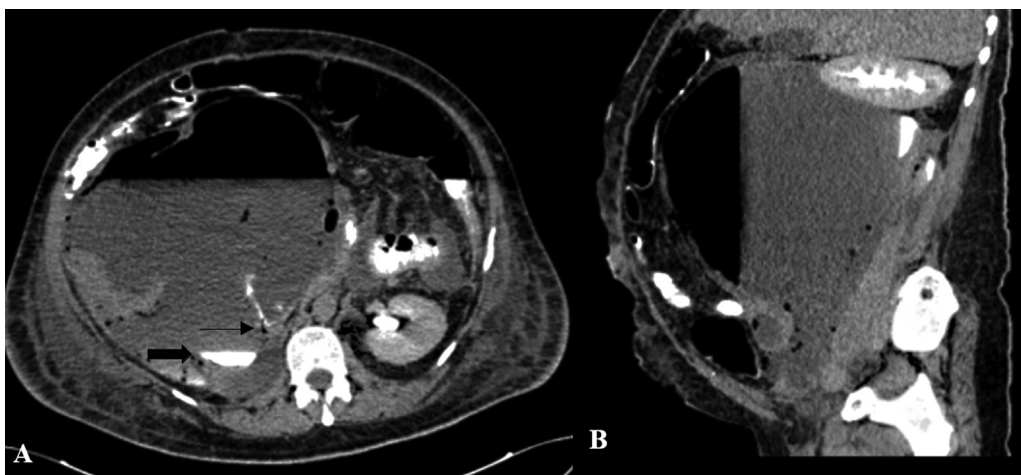


Fig. 12 (A) Axial contrast-enhanced computed tomography (CT) of the abdomen in 15-minute delayed phase in a 51-year-old woman with a history of abdominal surgery shows a large well-defined collection in the perinephric space. There is contrast spurt from the right ureter (*thin arrow* in A) and subsequent contrast layering in collection (*arrow* in A) resulting in the formation of *urinoma* secondary to ureteric injury. (B) Sagittal reformatted CT image shows cranial displacement of the right kidney.

as well-defined lesions of fluid attenuation in the retroperitoneum, more commonly in the perirenal space. On CT, they are seen as well-circumscribed fluid collections showing increasing attenuation caused by contrast-enhanced urine entering the urinoma on excretory phases (–Fig. 12).²⁵

Conclusions

Primary retroperitoneal masses are a rare group of neoplasms. They pose a diagnostic dilemma on imaging due to their varied and overlapping appearances. Imaging features in combination with demographic and clinical information help in narrowing down the differential diagnosis. CT has the advantage of being easily available and has a short acquisition time. CT is valuable in characterizing these lesions, in evaluating their extent and relations with surrounding structures, which is useful for surgical planning.

Funding

None.

Conflict of Interest

None declared.

References

- Coffin A, Boulay-Coletta I, Sebbag-Sfez D, Zins M. Radioanatomy of the retroperitoneal space. *Diagn Interv Imaging* 2015;96(02):171–186
- Chinwan D, Vohra P. Role of multidetector computed tomography in evaluation of retroperitoneal masses. *Int J Res Med Sci* 2018;6(12):3949–3953
- Rajiah P, Sinha R, Cuevas C, Dubinsky TJ, Bush WH Jr, Kolokythas O. Imaging of uncommon retroperitoneal masses. *Radiographics* 2011;31(04):949–976
- Mota MMDS, Bezerra ROF, Garcia MRT. Practical approach to primary retroperitoneal masses in adults. *Radiol Bras* 2018;51(06):391–400
- Scali EP, Chandler TM, Heffernan EJ, Coyle J, Harris AC, Chang SD. Primary retroperitoneal masses: what is the differential diagnosis? *Abdom Imaging* 2015;40(06):1887–1903
- Yu RS, Zhang WM, Liu YQ. CT diagnosis of 52 patients with lymphoma in abdominal lymph nodes. *World J Gastroenterol* 2006;12(48):7869–7873
- Manzella A, Borba-Filho P, D'Ippolito G, Farias M. Abdominal manifestations of lymphoma: spectrum of imaging features. *ISRN Radiol* 2013;2013:483069
- Shaaban AM, Rezvani M, Tubay M, Elsayes KM, Woodward PJ, Menias CO. Fat-containing retroperitoneal lesions: imaging characteristics, localization, and differential diagnosis. *Radiographics* 2016;36(03):710–734
- Craig WD, Fanburg-Smith JC, Henry LR, Guerrero R, Barton JH. Fat-containing lesions of the retroperitoneum: radiologic-pathologic correlation. *Radiographics* 2009;29(01):261–290
- Murphey MD, Arcara LK, Fanburg-Smith J. From the archives of the AFIP: imaging of musculoskeletal liposarcoma with radiologic-pathologic correlation. *Radiographics* 2005;25(05):1371–1395
- Angervall L, Kindblom LG, Merck C. Myxofibrosarcoma. A study of 30 cases. *Acta Pathol Microbiol Scand [A]* 1977;85A(02):127–140
- Lefkowitz RA, Landa J, Hwang S, et al. Myxofibrosarcoma: prevalence and diagnostic value of the “tail sign” on magnetic resonance imaging. *Skeletal Radiol* 2013;42(06):809–818
- Waters B, Panicek DM, Lefkowitz RA, et al. Low-grade myxofibrosarcoma: CT and MRI patterns in recurrent disease. *AJR Am J Roentgenol* 2007;188(02):W193–8
- Rha SE, Byun JY, Jung SE, Chun HJ, Lee HG, Lee JM. Neurogenic tumors in the abdomen: tumor types and imaging characteristics. *Radiographics* 2003;23(01):29–43
- Papaioannou G, McHugh K. Neuroblastoma in childhood: review and radiological findings. *Cancer Imaging* 2005;5(01):116–127
- Xu Y, Wang J, Peng Y, Zeng J. CT characteristics of primary retroperitoneal neoplasms in children. *Eur J Radiol* 2010;75(03):321–328
- Dumba M, Jawad N, McHugh K. Neuroblastoma and nephroblastoma: a radiological review. *Cancer Imaging* 2015;15(01):5
- Somarouthu BS, Shinagare AB, Rosenthal MH, et al. Multimodality imaging features, metastatic pattern and clinical outcome in adult extraskeletal Ewing sarcoma: experience in 26 patients. *Br J Radiol* 2014;87(1038):20140123
- Outwater EK, Siegelman ES, Hunt JL. Ovarian teratomas: tumor types and imaging characteristics. *Radiographics* 2001;21(02):475–490
- Guinet C, Buy JN, Ghossain MA, et al. Fat suppression techniques in MR imaging of mature ovarian teratomas: comparison with CT. *Eur J Radiol* 1993;17(02):117–121
- Friedman AC, Pyatt RS, Hartman DS, Downey EF Jr, Olson WB. CT of benign cystic teratomas. *AJR Am J Roentgenol* 1982;138(04):659–665
- Bazot M, Cortez A, Sananes S, Boudghène F, Uzan S, Bigot J-M. Imaging of dermoid cysts with foci of immature tissue. *J Comput Assist Tomogr* 1999;23(05):703–706
- Aronowitz J, Estrada R, Lynch R, Kaplan AL. Retroconversion of malignant immature teratomas of the ovary after chemotherapy. *Gynecol Oncol* 1983;16(03):414–421
- Moskovic E, Jobling T, Fisher C, Wiltshaw E, Parsons C. Retroconversion of immature teratoma of the ovary: CT appearances. *Clin Radiol* 1991;43(06):402–408
- Goenka AH, Shah SN, Remer EM. Imaging of the retroperitoneum. *Radiol Clin North Am* 2012;50(02):333–355, vii
- Al-Dasuqi K, Irshaid L, Mathur M. Radiologic-pathologic correlation of primary retroperitoneal neoplasms. *Radiographics* 2020;40(06):1631–1657
- Loke TK, Yuen NW, Lo KK, Lo J, Chan JC. Retroperitoneal ancient schwannoma: review of clinico-radiological features. *Australas Radiol* 1998;42(02):136–138